

Transport and Recovery of Bacteriophage PRD1 in a Sand and Gravel Aquifer: Effect of Sewage-Derived Organic Matter

ANN P. PIEPER,[†] JOSEPH N. RYAN,^{*,†}
RONALD W. HARVEY,[‡] GARY L. AMY,[†]
TISSA H. ILLANGASEKARE,[†] AND
DAVID W. METGE[‡]

Civil, Environmental, and Architectural Engineering
Department, University of Colorado, Boulder, Colorado 80309,
and U.S. Geological Survey, Water Resources Division,
3215 Marine Street, Boulder, Colorado 80303

To test the effects of sewage-derived organic matter on virus attachment, ³²P-labeled bacteriophage PRD1, linear alkylbenzene sulfonates (LAS), and tracers were injected into sewage-contaminated (suboxic, elevated organic matter) and uncontaminated (oxic, low organic matter) zones of an iron oxide-coated quartz sand and gravel aquifer on Cape Cod, MA. In the uncontaminated zone, 83% of the PRD1 were attenuated over the first meter of transport by attachment to aquifer grains. In the contaminated zone, 42% of the PRD1 were attenuated over the first meter of transport. Sewage-derived organic matter contributed to the difference in PRD1 attenuation by blocking attachment sites in the contaminated zone. At greater distances down-gradient (to a total transport distance of 3.6 m), a near-constant amount of PRD1 continued to break through, suggesting that aquifer grain heterogeneities allowed a small amount of reversible attachment. Injection of an LAS mixture (25 mg L⁻¹), a common sewage constituent, remobilized 87% of the attached PRD1 in the contaminated zone, but only 2.2% in the uncontaminated zone. LAS adsorption promoted virus recovery in the contaminated zone by altering the PRD1-surface interactions; however, the amount of LAS adsorbed was not sufficient to promote release of the attached PRD1 in the uncontaminated zone.

Introduction

The subsurface transport of pathogenic viruses from septic systems, leaking sewage lines, and sewage infiltration beds to water supply wells is controlled by attachment to aquifer sediments and inactivation (1, 2). Virus attachment depends on the solution chemistry of the groundwater and the surface chemistry of the virus and aquifer grains. Generally, virus attachment is favored by low pH and high ionic strength, conditions that reduce the electrostatic repulsive forces between virus and aquifer grain surfaces (3-6). Mineral phases characterized by positive surface charge (e.g., ferric oxyhydroxides) at pH values typical of most drinking water aquifers also promote extensive virus attachment through electrostatic attraction because the surfaces of most viruses

are negatively charged in natural waters (7-9). Organic matter, both in the aquatic and mineral-bound phases, plays an important role in virus transport by altering the interactions between viruses and aquifer grains. Some researchers have concluded that organic matter enhances virus transport by blocking virus attachment to mineral surfaces (10-14), while others suggest that organic matter inhibits virus transport by promoting hydrophobic interactions between the virus and grain surfaces (15-17). Viruses are typically introduced to the subsurface in the presence of high concentrations of sewage-derived organic matter; therefore, understanding of the effect of organic matter on virus transport is important in assessing the risks associated with virus contamination.

To test the effect of sewage-derived organic matter on virus transport, we injected bacteriophage PRD1, a virus that infects only specific strains of *Salmonella* bacteria, into an unconfined sand and gravel aquifer and monitored their transport over a distance of 3.6 m using multi-level samplers (MLSs). The aquifer, located downstream of sewage infiltration beds at the Massachusetts Military Reservation, Cape Cod, MA, has been the site of recent investigations of bacteria and virus transport experiments (18-21). The aquifer has been partially contaminated by the infiltrating sewage, producing two geochemically different zones: a contaminated zone (pH 6.0-6.7, high ionic strength, and high organic matter) and an overlying uncontaminated zone (pH 5.0-5.7, low ionic strength, and low organic matter). The PRD1 injection was followed by an injection of a mixture of linear alkylbenzene sulfonate (LAS) surfactant during which we monitored PRD1 recovery from the aquifer.

The bacteriophage PRD1 was selected for these field experiments because it has been used as a surrogate for transport behavior of water-borne viral pathogens (poliovirus, hepatitis A, rotavirus) in many laboratory and field studies (15-17, 21). Following procedures outlined by Murray and Laband (22), the genetic material of PRD1 was radiolabeled with ³²P to allow differentiation between attachment and inactivation of the PRD1. The LAS surfactants, injected at a concentration of 25 mg L⁻¹, are common detergent constituents often found in sewage effluents at this concentration (23-25).

Reported episodes of virus contamination of groundwater supplies indicate that viruses have been transported distances of tens to hundreds of meters in aquifers (26, 27), but recent field experiments have begun to identify key factors controlling virus transport—solution chemistry, aquifer mineralogy, and preferential flow through heterogeneities and fractures (21, 28-31). So far, field experiments have monitored virus transport by measuring only the infective virus population, yielding valuable estimates of public health risks, but less information on the underlying processes that control virus transport. Our field tests extend understanding of virus transport in groundwater by (1) monitoring the transport of the total virus population, not just the infective viruses, to isolate the effects of attachment on transport, (2) comparing transport in two geochemically different zones of the same aquifer, and (3) assessing the effect of high concentrations of sewage-derived organic matter on virus transport.

Experimental Section

Site Description. The virus injections were conducted in the surficial aquifer at the U.S. Geological Survey's Cape Cod Toxic Waste Research Site near the Massachusetts Military Reservation on Cape Cod, MA. The aquifer has been contaminated by disposal of secondary sewage effluent onto rapid infiltration sand beds for over 50 years (32), creating a

* Corresponding author address: University of Colorado, Campus Box 428, Boulder, CO 80309-0428; telephone: 303-492-0772; fax: 303-492-7317; e-mail: joe.ryan@colorado.edu.

[†] University of Colorado.

[‡] U.S. Geological Survey.

TABLE 1. Chemistry of Groundwater and Sediment in Unconfined Glacial Outwash Aquifer about 150 m Downstream of Sewage Infiltration Beds at the Massachusetts Military Reservation, Cape Code, MA^a

| constituent | units | contaminated zone | uncontaminated zone | refs |
|---------------------------------|------------------------|-------------------|---------------------|-----------|
| pH | | 6.0–6.7 | 5.0–5.7 | * |
| specific conductance | $\mu\text{S cm}^{-1}$ | 350–450 | 60–100 | * |
| Na ⁺ | μM | 1900 | 250 | 33 |
| K ⁺ | μM | 200 | 21 | 33 |
| Mg ²⁺ | μM | 130 | 37 | 33 |
| Ca ²⁺ | μM | 210 | 28 | 33 |
| NH ₄ ⁺ | μM | <1 | <1 | 33 |
| Fe (dissolved) | μM | 0.16 | <0.05 | 33 |
| Mn (dissolved) | μM | 15 | 0.64 | 33 |
| Cl ⁻ | μM | 760 | 230 | 33 |
| NO ₃ ⁻ | μM | 300 | <10 | 33 |
| SO ₄ ²⁻ | μM | 360 | 85 | 33 |
| HCO ₃ ⁻ | μM | 640 | 28 | 33 |
| PO ₄ ³⁻ | μM | 12 | 0.74 | 33 |
| dissolved oxygen | mg L ⁻¹ | 0–0.5 | 6–11 | *, 33, 38 |
| dissolved organic carbon | mg L ⁻¹ | 2.0–4.4 | 0.4–1.0 | 33, 38 |
| MBAS ^b | mg L ⁻¹ | 0.15 | 0.02 | *, 33 |
| surface Fe(III) ^c | $\mu\text{mol g}^{-1}$ | 3.6 ± 0.3 | 4.7 ± 1.4 | * |
| total Fe ^d | $\mu\text{mol g}^{-1}$ | 36 ± 15 | 38 ± 5 | * |
| sediment <i>f</i> _{oc} | | 0.01 | <0.0001 | 32, 38 |

^a Measurements by this study denoted by *. ^b MBAS, methylene blue active substances (detergents, surfactants). ^c Surface Fe(III) measured by Ti(III)–citrate–EDTA–bicarbonate reduction (46). ^d Total Fe measured by HF/HNO₃ digestion.

TABLE 2. Schedule of Injections and Initial Concentrations of Bacteriophage PRD1, LAS, and Tracers in the 100-L Injectates^a

| injection | duration (days) | aquifer zone | LAS | | |
|-----------|-----------------|--------------|------------------------------|----------------------------------|----------------------|
| | | | PRD1 (cpm mL ⁻¹) | surfactant (mg L ⁻¹) | tracer (mM) |
| I | 14 | uncontam | 3720 | | 1.9, Br ⁻ |
| | | contam | 2620 | | 1.9, Br ⁻ |
| Ia | 9 | uncontam | 257 | | 1.9, Br ⁻ |
| | | contam | 1470 | | 1.9, Br ⁻ |
| II | 16 | uncontam | | 25 | 4.2, Cl ⁻ |
| | | contam | | 25 | 4.2, Cl ⁻ |

^a PRD1 measured as ³²P-labeled PRD1 by radioassay. Injections Ia and II commenced one day after the conclusion of the preceding injections.

contaminant plume characterized by low dissolved oxygen concentrations and elevated pH, specific conductance, and organic carbon concentrations (Table 1). Previously, the site has been used to study the transport of groundwater tracers, metals, nutrients, detergents, microspheres, bacteria, protozoa, and viruses (18–21, 33–37).

The surficial aquifer consists of Pleistocene glacial outwash deposits characterized by interbedded lenses of sand and gravel (32, 33). The grains (average size 0.6 mm) consist mainly of quartz coated by crystalline ferric oxyhydroxides (38, 39). The effective porosity is 0.39, and the average hydraulic conductivity is 110 m d⁻¹. The water table depth is between 6 and 7 m below the surface near the study site. Measured groundwater velocities range from 0.3 to 1.0 m d⁻¹ (33).

Injections. Our initial plans called for two injections, PRD1 transport (injection I) and PRD1 recovery (injection II) (Table 2). An additional PRD1 transport experiment (injection Ia) was performed to attempt to collect samples for both total (radioassay) and infective (plaque assay) PRD1 concentrations; however, the bacterial host used in the plaque assay was not successfully prepared in the field laboratory during these injections. In each of these injections, the constituents were simultaneously injected into the up-gradient multi-level sampler (MLS) at two depths in the uncontaminated zone (6.4 and 6.7 m depths) and two depths in the contaminated zone (8.7 and 9.0 m depths) (Figure 1). The next injections were started when the bromide tracer from the previous

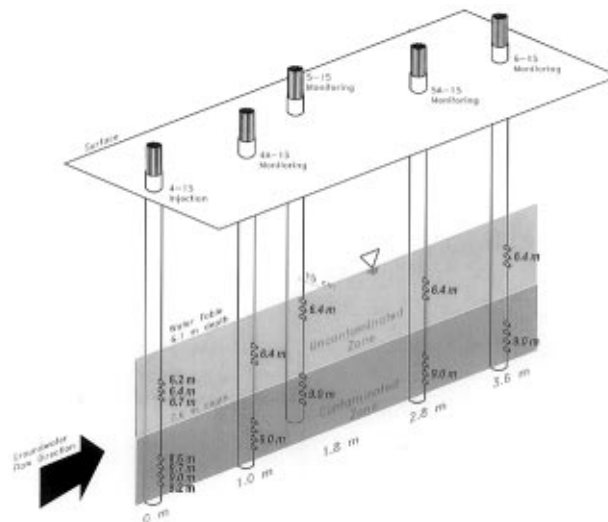


FIGURE 1. Multi-level sampler (MLS) array used to conduct the injections. Each MLS is a PVC pipe containing a bundle of 15 polyethylene tubes (0.64 cm diameter) that exit the PVC pipe at ports separation by 25 cm. The MLS located 1.8 m down-gradient of the injection MLS is located about 15 cm off the line formed by the other four MLSs. The transport distances, the depths below the surface, the approximate depths to the water table, and the transition between the uncontaminated and contaminated zones of the aquifer are noted. The injection depths (6.4, 6.7, 8.7, and 9.0 m) and the monitoring depths receiving most of the injectate mass (6.4 and 9.0 m) are italicized.

injection broke through at the sampling MLS furthest down-gradient (3.6 m transport distance).

For injections into the oxic uncontaminated zone, we first removed groundwater from the ports at 6.4 and 6.7 m depths of the up-gradient injection MLS into an open, acid-cleaned 115-L polyethylene vessel using two peristaltic pumps. The injection constituents were added to the uncontaminated groundwater to make a total of 100 L of injectate and stirred to mix with an acrylic tube. For injections into the suboxic (<0.3 mg L⁻¹ O₂) contaminated zone, we removed groundwater from the ports at 8.7 and 9.0 m depths of the up-gradient injection MLS into a collapsed, gas-impermeable, acid-cleaned, N₂-sparged 100-L fuel bladder (Aero Tech Lab;

Ramsey, NJ) without introducing air. The injection constituents were added when the bladder was about one-quarter full and mixed by agitating the bladder. The two 100-L injectates were then simultaneously pumped back into the same depths from which they were removed at a flow rate of about 1.0 L min⁻¹ for about 1.7 h.

Sampling. We sampled seven depths in four MLSs located down-gradient of the injection MLS (Figure 1). Immediately before and after the injections, we sampled all depths of the injection and monitoring MLSs to measure background and initial concentrations (C_0) for each constituent. Daily samples were collected at a rate of about 200 mL min⁻¹ by connecting peristaltic pump tubing (Norprene) directly to the MLS tubes (polyethylene). Following purging of about 200–300 mL of water standing in the MLS tubes, pH (pH paper, J.T. Baker Inc.), dissolved oxygen (CHEMet-kits, CHEMetrics, Inc.), specific conductance, and temperature (Checkmate 90 meter, Corning, Inc.) were measured for each sample (average values reported in Table 1). Samples were collected in polyethylene bottles pre-rinsed with a small amount of the sample groundwater and stored on ice in coolers in the field.

In the uncontaminated zone, the tracer transport velocity ranged from 0.8 to 1.3 m d⁻¹. In the contaminated zone, the tracer transport velocity was 0.4–0.7 m d⁻¹. Significant breakthrough of the injected constituents occurred in five of the seven MLS depths monitored. The breakthroughs representing the greatest mass of the constituents injected occurred at depths of 6.4 m in the uncontaminated zone and of 9.0 m in the contaminated zone (Figure 1). Our description of the transport behavior of the injected constituents will be limited to breakthroughs measured at these two depths. Complete breakthrough data are available in Pieper (40).

Tracers. We used 1.9×10^{-3} M NaBr as the conservative tracer for injections I and Ia and 4.2×10^{-3} M NaCl for injection II (to avoid overlapping bromide plumes). Bromide concentration was measured using a bromide-specific electrode (Orion 9435), a reference electrode (Beckman 39841), and a Beckman Φ 12 pH/ISE meter. Chloride concentration was measured using a combination chloride-specific electrode (Orion 961713). Error for replicate samples was less than 5% for these measurements. The relative detection limit of the bromide and chloride analyses was $C/C_0 = 0.0067$.

Virus. The bacteriophage PRD1 is characterized by a diameter of 62 nm, a $\text{pH}_{\text{iep}} < 4$ in a calcium-phosphate solution (15), and a hydrophobic lipid layer (1). It is similar in size and surface character to many enteroviruses (41), and its inactivation rate in groundwater is relatively slow (42, 43). The radiolabeled PRD1 stocks were prepared following methods outlined in Loveland et al. (9). Before injection, the virus stock was extensively purified to remove organic matter and unincorporated ³²P by rate-zonal ultracentrifugation. Fractions in which the ³²P label and the infective viruses coincided were pooled and resuspended in phosphate buffer solution for addition to the injectate. The initial virus concentrations varied considerably from injection to injection (Table 2).

Samples were shipped every 5 days to the USGS laboratory in Boulder, CO, mixed with scintillation cocktail (Packard Ultima Gold), and measured by liquid scintillation counting (Beckman LS3801). All ³²P count rates were adjusted for the background count rate (110 ± 4 counts min⁻¹) and radioactive decay. Error between replicate samples for this method was about 10%. The relative detection limit of this method was $C/C_0 = 0.002$ – 0.031 depending on the ³²P-PRD1 C_0 value.

The total PRD1 number concentration of the ³²P-labeled stocks was estimated by measuring the optical density of the PRD1 stocks at $\lambda = 260$ nm and relating it to the extinction coefficient for the proteins in virus capsids (22). Following this technique, a ³²P count rate of 1 count min⁻¹ corresponded to 30 and 35 PRD1 viruses for the two PRD1 stock suspen-

sions. The error in this relationship between ³²P count rate and total PRD1 number concentration was estimated at 30%.

Linear Alkylbenzene Sulfonates. The LAS mixture added to the injectate is comprised of isomers with aliphatic chains ranging from C₁₀ to C₁₄ and average molecular mass of 325.5 Da. The mixture is classified as 50.5% active (i.e., 50.5% by weight of the mixture is LAS isomers; 47.4% water, 1.2% neutral oils, and 0.9% sulfate) by its supplier, Vista Chemical Co. (Alston, TX). The oils contained in this mixture are unsulfonated linear alkylbenzenes and bis(alkylphenyl) sulfones. The injectate concentration of the LAS was 7.7×10^{-5} M (25 mg L⁻¹), or about 5% of the critical micelle concentration (cmc) of a similar commercial LAS mixture containing neutral oils, 1.4×10^{-3} M (44). LAS concentration was usually measured immediately upon return to the field laboratory using methylene blue active substances (MBAS) kits for measuring detergents (CHEMetrics, Inc.). When it was not possible to perform the MBAS analysis immediately, samples were preserved by adding 2.5 mL of formalin to each sample to avoid biodegradation. Background MBAS concentration in the aquifer never exceeded 0.5 mg L⁻¹. The error for this procedure was 15% among replicate samples. The relative detection limit for LAS was $C/C_0 = 0.010$.

Ferric Oxyhydroxide Coatings. Continuous vertical cores were retrieved about 15 m east of the injection array for measurement of the total Fe and “surface” Fe(III) in ferric oxyhydroxide coatings. Owing to the density of the MLS array, cores could not be obtained closer to the injection array. The cores were recovered using a hollow stem auger and an *in situ* quick-freeze technique that uses liquid CO₂ to freeze a plug of sediment at the bottom of the sampling tube to retain pore water (45). The cores were collected in acrylic tubes that were capped, sealed with tape, and shipped in coolers to the University of Colorado where they were sectioned into 40–60 cm lengths and stored at 4 °C. Pore water was extracted from each core section and measured for pH and specific conductance to identify the core section as uncontaminated or contaminated. Samples from three uncontaminated and three contaminated core sections were measured for surface Fe(III) by the Ti(III)–citrate–EDTA–bicarbonate method (46) and for total Fe by HF/HNO₃ digestion in heated Teflon-lined bombs in duplicate or triplicate analyses. The iron concentrations were measured by inductively coupled argon plasma atomic emission spectroscopy (Varian Liberty 150 AX Turbo). Error in replicate samples was less than 20%.

Calculation of Retardation, Attenuation, Collision Efficiency, and Recovery. Retardation factors (RF) for PRD1 and LAS were calculated as the ratios of time required to reach the maximum dimensionless concentrations at down-gradient MLSs to that for the tracers. Estimates of retardation factors are only approximate due to the sampling interval (daily) and peak concentrations near the lower detection limit, the background ³²P count rate.

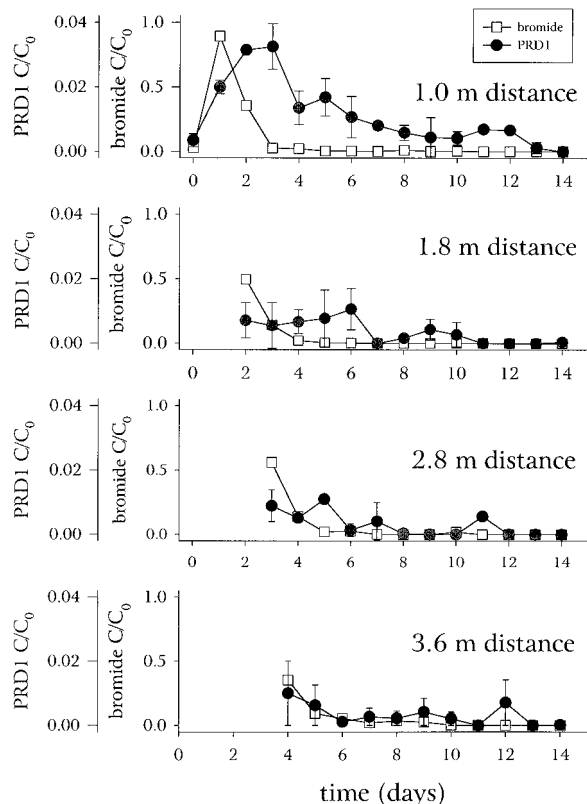
The relative breakthrough (RB) of an injected constituent is a comparison of the time-integrated mass of the constituent relative to that of the conservative tracer (18):

$$\text{RB (\%)} = \left[\frac{\int_{t_0}^{t_f} [C]_t dt}{\int_{t_0}^{t_f} [C]_0 dt} \right] \times 100 \quad (1)$$

where $[C]_0$ is the PRD1 or LAS concentration in the injection MLS, $[C]_t$ is the bromide or chloride concentration in the injection MLS, $[C]_t$ and $[\text{tracer}]_t$ are the concentrations at time t , and t_0 and t_f are the times of the beginning and end of breakthrough. The attenuation (%) of an injected constituent is $100 - \text{RB}$.

The collision efficiency, α , the ratio of the rate of collisions resulting in attachment to the total rate of collisions between

a. Injection I Uncontaminated Zone



b. Injection I Contaminated Zone

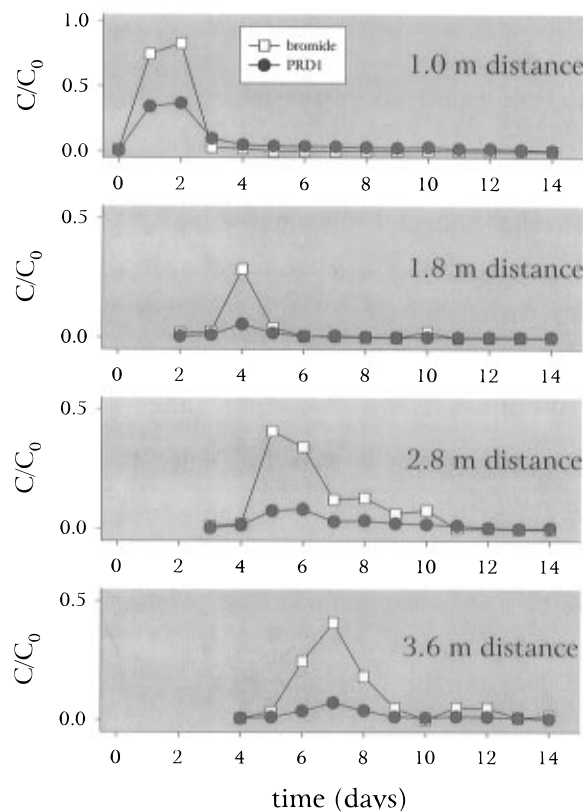


FIGURE 2. Injection I breakthrough curves at the four transport distances for PRD1 (^{32}P -labeled) and bromide: (a) uncontaminated zone (depth 6.4 m) and (b) contaminated zone (depth 9.0 m). The constituent and tracer concentrations were normalized to their concentrations at the same depth in the injection well on day 0. During injection I, the tracer traveled faster than anticipated in the uncontaminated zone. Injection Ia breakthrough curves displayed similar characteristics. Breakthrough at 1.8 m transport distance is small because the MLS is located slightly off the gradient direction. Error bars show the range of samples analyzed twice.

particles and collector grains, was calculated for the pulse input of PRD1 as (19)

$$\alpha = \frac{d[[1 - 2(\alpha_L/x) \ln(\text{RB})]^2 - 1]}{6(1 - \theta)\eta\alpha_L} \quad (2)$$

where d is the average grain diameter (0.6 mm), α_L is the longitudinal dispersivity (m), x is the transport distance (the down-gradient distance of the monitoring MLS), θ is the porosity (0.39), and η is the single collector efficiency (47, 48). The longitudinal dispersivity was calculated as (19)

$$\alpha_L = \frac{x(\Delta t/t_{\text{peak}})^2}{16 \ln 2} \quad (3)$$

where Δt is the time (days) during which $[\text{PRD1}]_t > 1/2[\text{PRD1}]_{\text{max}}$ and t_{peak} is the time to peak concentration (days). The α_L value calculated for uncontaminated zone during injection Ia was used for injection I because complete breakthrough curves were not sampled. The single collector efficiency of PRD1 was calculated using only the Brownian diffusion contribution to η (48) because the deposition of sub-micrometer particles is dominated by Brownian diffusion:

$$\eta = 0.9A_s^{1/3} \left(\frac{k_B T}{\mu d_p dv} \right)^{2/3} \quad (4)$$

where A_s is the Happel sphere-in-cell model correction factor, k_B is the Boltzmann constant ($1.38 \times 10^{-23} \text{ J mol}^{-1} \text{ K}^{-1}$), T is the absolute temperature (288 K), μ is the dynamic viscosity of the fluid ($1.139 \times 10^{-3} \text{ kg m}^{-1} \text{ s}^{-1}$), d_p is the PRD1 diameter

($6.2 \times 10^{-8} \text{ m}$), d is the average grain diameter, and v is the fluid velocity for the uncontaminated (1.0 m s^{-1}) and contaminated (0.5 m s^{-1}) zones. The Happel correction factor, for $\epsilon = (1 - \theta)^{1/3}$, is (48)

$$A_s = \frac{1 - \epsilon^5}{1 - 1.5\epsilon + 1.5\epsilon^5 - \epsilon^6} \quad (5)$$

The recovery (%) of PRD1 by LAS was estimated as the amount of PRD1 recovered during injection II divided by the amount of PRD1 attenuated during injections I and Ia. The amount attenuated over the first meter of transport was calculated as the difference between the amount injected and the amount appearing at the 1.0 m transport distance integrated over time and summed for injections I and Ia. The amount of PRD1 recovered during injection II was calculated as the amount appearing at the 1.0 m transport distance integrated over time for each depth.

Results

Injections I and Ia, PRD1 Transport. In the uncontaminated zone, most of the PRD1 was attenuated over the first 1.0 m of transport (Figure 2, Table 3). The unattenuated PRD1 migrated through the contaminated zone at approximately the same velocity as the bromide tracer. Far less PRD1 was attenuated in the contaminated zone than in the uncontaminated zone. The relative breakthroughs decreased over the first 1.8 m of transport distance, but they remained nearly constant over the remaining 1.8 m of transport distance (Figure 3). The amount of ^{32}P -labeled PRD1 added in injection Ia was substantially less than that added in injection I (Table 2), but the results were qualitatively similar.

TABLE 3. Retardation Factors (RFs), Maximum Concentrations, Relative Breakthroughs (RBs), Attenuations, and Collision Efficiencies (α) for PRD1 at 1.0 m Transport Distance^a

| constituent | injection no. | aquifer zone | RF | (C/C_0) _{max} at 1.0 m | RB at 1.0 m (%) | attenuation at 1.0 m (%) | α at 1.0 m |
|-------------|---------------|--------------|-----------------|-------------------------------------|-----------------|--------------------------|-------------------|
| PRD1 | I | uncontam | nd ^b | 0.033 | 12 | 88 | 0.013 |
| | | contam | 1.0 | 0.097 | 67 | 33 | 0.0014 |
| PRD1 | Ia | uncontam | 1.0 | 0.06 | 22 | 78 | 0.009 |
| | | contam | 1.0 | 0.15 | 50 | 50 | 0.0026 |
| LAS | II | uncontam | 1.0 | 0.75 | 86 | 14 | na ^c |
| | | contam | 1.0 | 0.71 | 88 | 12 | na |

^a RB values calculated using eq 1. Attenuation calculated as 100 - RB (%). Collision efficiency calculated using eq 2. Uncontaminated zone results were obtained at a depth of 6.4 m; contaminated zone results were obtained at a depth of 9.0 m. ^b nd, not determined with available data owing to very low PRD1 concentrations. ^c na, not applicable.

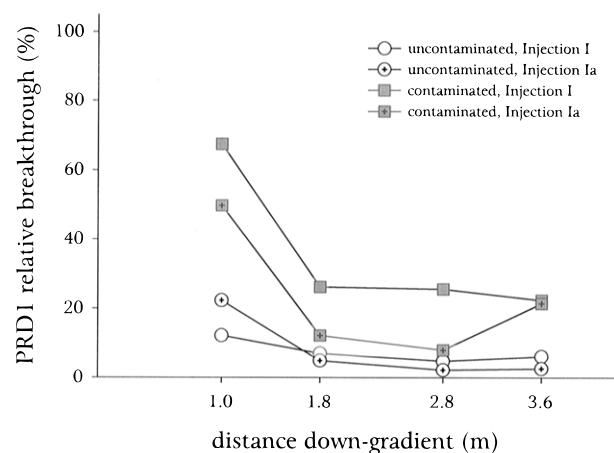


FIGURE 3. Relative breakthrough of PRD1 in uncontaminated and contaminated zones as a function of distance down-gradient during injections I and Ia.

Injection II, PRD1 Recovery. In the uncontaminated zone, injection of LAS recovered 2.2% of the PRD1 attached over the first meter of transport (Figure 4). In the contaminated zone, LAS flushing recovered 87% of the PRD1 attenuated over the first 1.0 m of transport distance. Breakthrough of the LAS was approximately coincident with the breakthrough of the chloride tracer in both zones (Figure 4). The attenuation of LAS was approximately the same, 14 and 12%, in the uncontaminated and contaminated zones (Table 3). In the contaminated zone, the appearance of released PRD1 coincided with the appearance of chloride and LAS at the 1.0 m transport distance; however, PRD1 concentration decreased slowly after the passage of the LAS plume.

Ferric Oxyhydroxide Coatings. The surface Fe(III) and total Fe concentrations of the uncontaminated and contaminated core sections were not significantly different (Table 1). About 10–12% of the total Fe is surface Fe(III) in both cores. The surface Fe(III) and total Fe concentrations measured are similar to those measured by Scholl and Harvey (38) and Coston et al. (39) at the Cape Cod site.

Discussion

PRD1 Transport and Attachment. About three times more PRD1 migrated through the first meter of the contaminated zone than through the first meter of the uncontaminated zone. PRD1 that eluded attachment traveled at the same rate as the bromide tracer in both zones; thus, PRD1 transport was limited mainly by attenuation and not retardation. The attenuation can be attributed to attachment that can be considered predominantly irreversible with respect to the chemical conditions of the aquifer and the time scale of the experiment. We surmise that the greater breakthrough of PRD1 through the contaminated zone, reflected by the lower collision efficiencies (Table 3), can be attributed primarily to

elevated organic matter concentrations in the contaminated zone.

In the uncontaminated zone, it is likely that the PRD1 attenuation was caused by electrostatic attraction between oppositely charged PRD1 and ferric oxyhydroxide surfaces. Based on the measured pH_{iep} values, the PRD1 surface should be negatively charged (15) and the ferric oxyhydroxide coatings on the quartz grains should be positively charged (49) at the pH of the uncontaminated groundwater, about 5.5. In experiments designed to simulate PRD1 interactions with the Cape Cod aquifer material, PRD1 attached to quartz grains coated by ferric oxyhydroxides below pH 7.5, but not above (9, 50). Extensive attachment of bacteria to ferric oxyhydroxide coatings has also been observed at pH values below 7–8 (38, 51, 52).

The difference in PRD1 transport between the contaminated and uncontaminated zones may be affected by five differences in the groundwater chemistry caused the infiltration of treated sewage: (1) higher organic matter content, (2) higher phosphate and sulfate concentrations, (3) higher pH, (4) higher ionic strength, and (5) higher bivalent cation concentrations. Higher organic matter concentrations would enhance PRD1 transport by blocking virus attachment sites (10–14) or inhibit PRD1 transport by promoting hydrophobic interactions (15–17). Higher phosphate concentrations and pH would enhance PRD1 transport, while higher ionic strength and bivalent cation concentrations would inhibit PRD1 transport.

The higher organic matter content of the contaminated zone—2–11 times as much dissolved organic carbon and at least 100 times as much sediment organic carbon—appeared to play the dominant role in enhancing PRD1 transport. Natural forms of organic matter adsorb strongly to ferric oxyhydroxides primarily by surface complexation (53, 54), leading to colloidal stability of ferric oxyhydroxide suspensions through charge reversal at very low concentrations (≤ 1 mg L^{-1}) (55–57). Most of the dissolved organic matter near the sewage infiltration beds is poorly characterized (23, 25), so it is difficult to quantify its effect on ferric oxyhydroxide surface charge. In most cases, however, the addition of sewage-derived organic matter to virus suspensions is effective in enhancing virus transport through porous media (14, 58). The additional organic matter in the contaminated zone apparently did not promote attachment of viruses to aquifer grains by hydrophobic interaction as proposed by Kinoshita et al. (17).

Phosphate and sulfate, present at elevated concentrations in the contaminated zone, could also have contributed to enhanced PRD1 transport. Liang and Morgan (59) showed that relatively low phosphate concentrations were capable of reversing the surface charge of hematite suspensions; however, adsorption of organic matter on hematite achieves charge reversal at lower surface coverages (55). Typically, sulfate is less effective than phosphate at causing charge reversal; therefore, we expect that organic matter is the major factor in enhancing PRD1 transport.

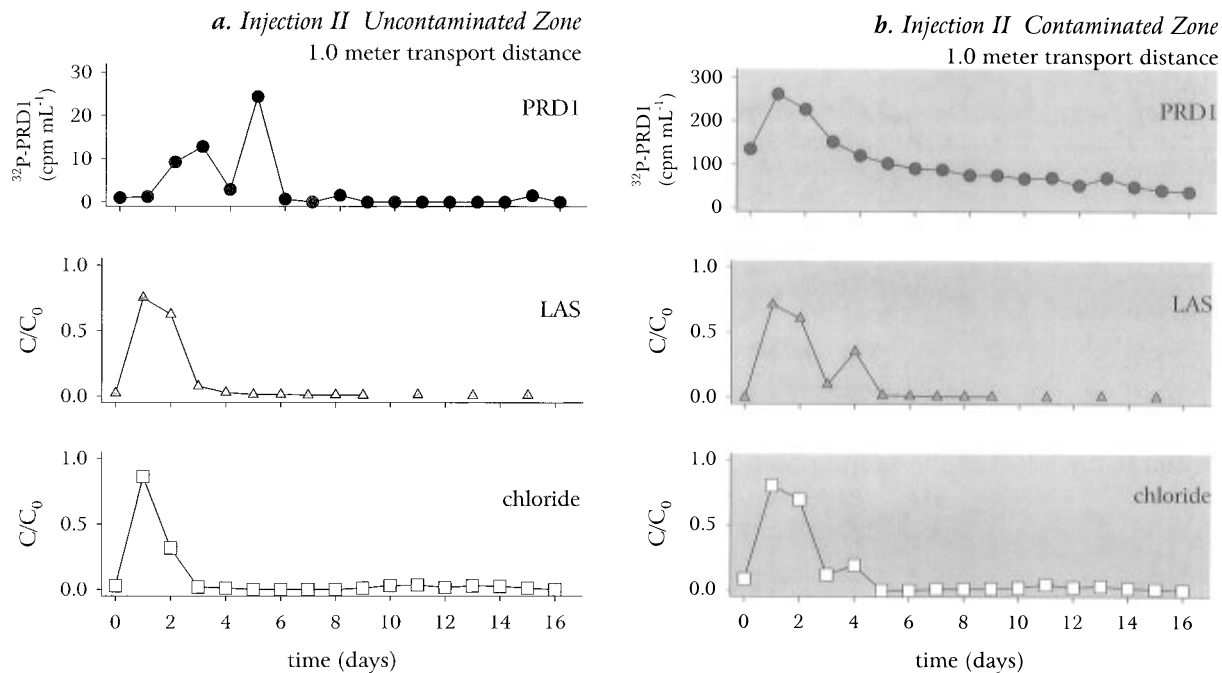


FIGURE 4. Injection II breakthrough and recovery curves at the 1.0 m transport distance for PRD1 (³²P-labeled), LAS, and chloride in (a) the uncontaminated zone (depth 6.4 m) and (b) the contaminated zone (depth 9.0 m). The PRD1 concentration is presented as the background- and decay-adjusted ³²P count rate per sample volume (cpm mL⁻¹). The LAS and tracer concentrations were normalized to their concentrations at the same depth in the injection well on day 0.

The average pH of the contaminated groundwater, about 6.2, is slightly higher than the average pH of the uncontaminated groundwater, about 5.5. A pH increase from 5.5 to 6.2 will decrease the positive charge on ferric oxyhydroxides, but it should not cause charge reversal because the pH of the contaminated groundwater is still below the pH_{iep} of ferric oxyhydroxides, about 7–8. Therefore, the pH increase is unlikely to have enhanced the PRD1 transport significantly.

The ionic strength and bivalent cation concentrations of the contaminated groundwater are about 4–7 times greater than those in the uncontaminated groundwater. Increases in ionic strength and bivalent cation concentrations generally increase the extent of virus attachment through double-layer compression and shielding of repulsive interactions (4, 60, 61). However, the enhanced PRD1 transport in the contaminated zone suggests that the presence of organic matter counteracted the effect of elevated ionic strength and bivalent cation concentration.

Comparison of Collision Efficiencies. The collision efficiencies measured for PRD1 transport (0.0014–0.013) are similar to those measured for the transport of other “biocolloids” at the Cape Cod site. Harvey and colleagues measured α values of 0.0054–0.0097 for indigenous bacteria of 0.4–0.7 μm diameter (18) and 0.026–0.069 for flagellated protozoa of 2–3 μm diameter (20). The relative value of the collision efficiencies should be a direct indicator of the intersurface forces experienced by each of these biocolloids as they approach the Cape Cod aquifer grains; however, details of the surface chemistry of the bacteria and protozoa (*i.e.*, pH_{iep}) are not available for comparison.

Our field-measured collision efficiencies for the PRD1 are much lower than the collisions efficiencies measured by Kinoshita et al. (17) for PRD1 attachment in laboratory columns containing the same Cape Cod sediments (α values of 0.59– \geq 0.94 over a pH range of 5.7–8.2). In the laboratory experiments, the PRD1 were suspended in solutions free of organic matter. The difference in the collision efficiencies suggests that even the low concentrations of dissolved natural organic matter in uncontaminated groundwater, 0.4–1.0 mg L⁻¹, enhanced PRD1 transport. The laboratory-measured

collision efficiencies were measured in a calcium–phosphate solution; however, the concentration of the calcium–phosphate solution was not given, so the effect of phosphate on the surface charge of the ferric oxyhydroxides cannot be determined.

Reversible Attachment and Surface Heterogeneity. We observed that the rate of attenuation of PRD1 over distance was not maintained during injections I or Ia (Figure 3). The plateau in the relative breakthroughs of PRD1 over distance suggests that either (1) a small fraction of the PRD1 virus population with anomalous surface properties resisted attachment or (2) a small fraction of the attached PRD1 was released after the major pulse passed. While the first possibility must be tested in future studies, the second possibility may be supported by the presence of patchy ferric oxyhydroxide coatings on the quartz grains (39). At the pH of the uncontaminated groundwater, about 5.5, attachment to the ferric oxyhydroxides is expected to be irreversible, but attachment to quartz is expected to be reversible (7, 9). Thus, it is possible that a small fraction of the PRD1 attached temporarily to uncoated patches of the quartz grains and was later released after the PRD1 plume passed. Bacteria transport through the Cape Cod aquifer has been modeled as a combination of irreversible and reversible attachment corresponding to deposition of bacteria in the primary minimum and secondary minimum of the DLVO (62, 63) potential energy between surfaces (19). It is possible that the irreversible and reversible bacteria attachment behavior was caused by bacteria attachment to heterogeneous grain surfaces. Recent advances in colloid deposition theory have included consideration of heterogeneous grain surfaces (64).

PRD1 Recovery by LAS. The addition of the LAS mixture remobilized most of the attached PRD1 in the contaminated zone (about 87%) but not in the uncontaminated zone (only 2.2%). It is unlikely that LAS directly affected the PRD1 surface charge (65); therefore, we anticipated that LAS would effectively remobilize PRD1 by affecting the surface charge of the ferric oxyhydroxide coatings. Laboratory experiments have shown that LAS adsorption can cause reversal of surface charge on aluminum oxides (66–69). Without direct evidence

of surface charge in the aquifer, we must surmise that the amount of LAS injected into the uncontaminated zone was insufficient to cause charge reversal; hence, only a very small amount of the PRD1 was mobilized. On the other hand, the LAS injected into the contaminated zone appears to have been sufficient to cause complete charge reversal because the many of the attachment sites on the ferric oxyhydroxides must have already been blocked by adsorbed organic matter from the sewage plume.

In the uncontaminated zone, LAS moved through the aquifer at about the same rate as the chloride tracer, but about 14% of the LAS was attenuated over the first meter of transport, indicating that some adsorption of LAS occurred. Using estimates of the cross-sectional flow area around a single MLS port (625 cm², based on the 25 cm vertical separation distance between the MLS ports), the average amount of ferric oxyhydroxides (4.7 μmol g⁻¹; Table 1), and a typical surface area for natural goethites (50 m² g⁻¹; 70), we can roughly estimate the LAS adsorption density on the ferric oxyhydroxide coatings as about 1.9 × 10⁻⁸ mol m⁻². This adsorption density is less than that required for hemimicelle formation, the prerequisite for charge reversal, by LAS on alumina (67). Without charge neutralization or reversal, it is unlikely that the adsorption of LAS would have caused mobilization of the attached PRD1 in the uncontaminated zone.

The attenuation of LAS over the first meter of transport in the contaminated zone (12%) was slightly less than that attenuated in the uncontaminated zone; therefore, the adsorption density was also below that expected for hemimicelle formation and charge reversal. Nevertheless, LAS flushing resulted in near-complete recovery of the attached PRD1. We surmise that the addition of LAS to the contaminated zone effectively remobilized the attached PRD1 because fewer virus attachment sites exist in the contaminated plume due to the presence of substantial amounts of adsorbed organic matter.

The release of PRD1 was slow relative to the LAS breakthrough in the contaminated zone (Figure 4), suggesting that the adsorption of LAS (in addition to the organic matter already present) produced weak electrostatic repulsion between the attached PRD1 and grain surfaces. If the repulsion between the attached PRD1 and aquifer sediments were strong, we would expect that the PRD1 would have been released rapidly because the kinetics of colloid release from surfaces are theoretically related to the strength of the repulsive intersurface force (71, 72).

Implications for Virus Transport Modeling. The results of these field tests suggest that virus attachment to aquifer grains is primarily an irreversible process that can be adequately described by colloid filtration (47, 48). Because the colloid filtration model is limited to "clean bed" deposition, exceptions still must be made for situations involving the blocking of attachment by previously attached viruses and the heterogeneity of aquifer grain surfaces (64, 73). Current models of virus transport in groundwater (15, 16, 74–78) utilize a range of attachment processes from reversible partitioning to two-site reversible and irreversible attachment; however, the concurrent breakthrough of viruses with conservative tracers in this and other field experiments conducted in porous media (21, 28, 31) indicate that virus attachment to aquifer sediments is predominantly irreversible. The possible contribution of surface heterogeneity to reversible virus attachment, which may be responsible for the decreasing PRD1 removal with distance observed in this field test, merits further investigation. These results may also serve to emphasize that spatial or temporal changes in geochemical conditions during virus transport must also be considered in virus transport modeling.

The effect of organic matter in virus attachment must be considered for accurate prediction of virus transport times. To advance our ability to *a priori* predict the extent of virus

transport, two key needs must be addressed: (1) measurements of virus and aquifer grain surface properties and (2) better understanding of the relationship between virus and aquifer grain surface properties and the frequency with which virus collisions with aquifer grains result in attachments. The results of this research suggest that organic matter plays an important role in the surface properties of aquifer grain surfaces and, hence, in virus attachment. Because virus transport scenarios typically involve elevated concentrations of sewage-derived organic matter, the need to comprehend the role of organic matter on virus–aquifer grain interactions is acute.

Acknowledgments

The National Water Research Institute and the U.S. Environmental Protection Agency supported this research through Grant HRA-699-514-92. Philip Berger (EPA) provided insight into regulatory aspects of virus transport. Denis LeBlanc and Kathy Hess (USGS, Massachusetts District) arranged access to the field site and retrieval of the sediment cores. Charles Gerba (University of Arizona) supplied the PRD1 and host seed stocks. Jon Loveland (University of Colorado) prepared the virus stocks and performed the liquid scintillation counting. Karla Kirkegaard, Connie Nugent, and Mali Illan-gasekare (University of Colorado) provided technical assistance and equipment for the virus purification. Larry Barber (U.S. Geological Survey) provided the LAS mixture and assisted with the first injection. Dick Smith (U.S. Geological Survey) lent field equipment. Rebecca Ard (University of Colorado) measured the iron content of the sediment cores. Dave Kinner (University of New Hampshire), Patty Li (University of Colorado), Heather Reddy (University of Virginia), Shirley Steinmacher (U.S. Geological Survey), and Brigid Welch (Tulane University) assisted with sample collection and analysis in the field. Finally, Menachem Elimelech (UCLA) and two anonymous reviewers provided valuable critiques of the manuscript.

Literature Cited

- (1) Gerba, C. P. *Adv. Appl. Microbiol.* **1984**, *30*, 133.
- (2) Berger, P. In *Ground Water Contamination and Control*; Zoller, U., Ed.; Marcel Dekker: New York, 1994; p 645.
- (3) Goyal, S. M.; Gerba, C. P. *Appl. Environ. Microbiol.* **1979**, *38*, 241.
- (4) Sobsey, M. D.; Dean, C. H.; Knuckles, M. E.; Wagner, R. A. *Appl. Environ. Microbiol.* **1980**, *40*, 92.
- (5) Lipson, S. M.; Stotzky, G. *Appl. Environ. Microbiol.* **1983**, *46*, 673.
- (6) Zerda, K. S.; Gerba, C. P.; Hou, K. C.; Goyal, S. M. *Appl. Environ. Microbiol.* **1985**, *49*, 91.
- (7) Murray, J. P.; Parks, G. A. In *Particulates in Water: Characterization, Fate, Effects, and Removal*; Kavanaugh, M. C., Leckie, J. O., Eds.; ACS Advances in Chemistry Series 189; American Chemical Society: Washington, DC, 1980; pp 97–103.
- (8) Taylor, D. H.; Moore, R. S.; Sturman, L. S. *Appl. Environ. Microbiol.* **1981**, *42*, 976.
- (9) Loveland, J. P.; Ryan, J. N.; Amy, G. L.; Harvey, R. W. *Colloids Surf. A: Physicochem. Eng. Asp.* **1996**, *107*, 205.
- (10) Burge, W. D.; Enkiri, N. K. *J. Environ. Qual.* **1978**, *7*, 73.
- (11) Moore, R. S.; Taylor, D. H.; Sturman, L. S.; Reddy, M. M.; Fuhs, G. W. *Appl. Environ. Microbiol.* **1981**, *42*, 963.
- (12) Moore, R. S.; Taylor, D. H.; Reddy, M. M.; Sturman, L. S. *Appl. Environ. Microbiol.* **1982**, *44*, 852.
- (13) Fuhs, G. W.; Chen, M.; Sturman, L. S.; Moore, R. S. *Microb. Ecol.* **1985**, *11*, 25.
- (14) Powelson, D. K.; Simpson, J. R.; Gerba, C. P. *Appl. Environ. Microbiol.* **1991**, *57*, 2192.
- (15) Bales, R. C.; Hinkle, S. R.; Kroeger, T. W.; Stocking, K.; Gerba, C. P. *Environ. Sci. Technol.* **1991**, *25*, 2088.
- (16) Bales, R. C.; Li, S.; Maguire, K. M.; Yahya, M. T.; Gerba, C. P. *Water Resour. Res.* **1993**, *29*, 957.
- (17) Kinoshita, T.; Bales, R. C.; Maguire, K. M.; Gerba, C. P. *J. Contam. Hydrol.* **1993**, *14*, 55.
- (18) Harvey, R. W.; George, L. H.; Smith, R. L.; LeBlanc, D. R. *Environ. Sci. Technol.* **1989**, *23*, 51.
- (19) Harvey, R. W.; Garabedian, S. P. *Environ. Sci. Technol.* **1991**, *25*, 178.

- (20) Harvey, R. W.; Kinner, N. E.; Bunn, A.; MacDonald, D.; Metge, D. *Appl. Environ. Microbiol.* **1995**, *61*, 209.
- (21) Bales, R. C.; Li, S.; Maguire, K. M.; Yahya, M. T.; Gerba, C. P.; Harvey, R. W. *Ground Water* **1995**, *33*, 653.
- (22) Murray, J. P.; Laband, S. J. *Appl. Environ. Microbiol.* **1979**, *37*, 480.
- (23) Thurman, E. M.; Barber, L. B., II; LeBlanc, D. J. *Contam. Hydrol.* **1986**, *1*, 143.
- (24) Rapaport, R. A.; Eckhoff, W. S. *Environ. Toxicol. Chem.* **1990**, *9*, 1245.
- (25) Field, J. A.; Barber, L. B.; Thurman, E. M.; Moore, B. L.; Lawrence, D. L.; Peake, D. A. *Environ. Sci. Technol.* **1992**, *26*, 1140.
- (26) Keswick, B. H.; Wang, D.-S.; Gerba, C. P. *Ground Water* **1982**, *20*, 142.
- (27) Yates, M. V. *J. Am. Water Works Assoc.* **1995**, *87*, 76.
- (28) Havelaar, A. H.; van Olphen, M.; Schijven, J. F. Presented at the 7th Biannual International Conference of the International Association of Water Quality, Budapest, Hungary, July 1994.
- (29) McKay, L. D.; Cherry, J. A.; Bales, R. C.; Yahya, M. T.; Gerba, C. P. *Environ. Sci. Technol.* **1993**, *27*, 1075.
- (30) McKay, L. D.; Gillham, R. W.; Cherry, J. A. *Water Resour. Res.* **1993**, *29*, 3879.
- (31) Rossi, P.; De Carvalho-Dill, A.; Müller, I.; Aragno, M. *Environ. Geol.* **1994**, *23*, 192.
- (32) LeBlanc, D. R. *Water-Supply Paper 2218*; U.S. Geological Survey: Reston, VA, 1984.
- (33) LeBlanc, D. R.; Garabedian, S. P.; Hess, K. M.; Gelhar, L. W.; Quadri, R. D.; Stollenwerk, K. G.; Wood, W. W. *Water Resour. Res.* **1991**, *27*, 895.
- (34) Hess, K. M.; Wolf, S. H.; Celia, M. A. *Water Resour. Res.* **1992**, *28*, 2011.
- (35) Kent, D. B.; Davis, J. A.; Anderson, L. C. D.; Rea, B. A. *Water Resour. Res.* **1994**, *30*, 1099.
- (36) Smith, R. L.; Howes, B. L.; Garabedian, S. P. *Appl. Environ. Microbiol.* **1991**, *57*, 1997.
- (37) Barber, L. B., II; Krueger, C.; Metge, D. W.; Harvey, R. W.; Field, J. A. In *Surfactant-Enhanced Subsurface Remediation: Emerging Technologies*; Sabatini, D. A., Knox, R. C., Harwell, J. H., Eds.; ACS Symposium Series 594; American Chemical Society: Washington, DC, 1995; pp 95–111.
- (38) Scholl, M. A.; Harvey, R. W. *Environ. Sci. Technol.* **1992**, *26*, 1410.
- (39) Coston, J. A.; Fuller, C. C.; Davis, J. A. *Geochim. Cosmochim. Acta* **1995**, *59*, 3535.
- (40) Pieper, A. P. Virus Transport in Groundwater: A Natural-Gradient Field Experiment in a Contaminated Sandy Aquifer. M.S. Thesis, Department of Civil, Environmental and Architectural Engineering, University of Colorado, Boulder, 1995.
- (41) IAWPRC Study Group on Health Related Water Microbiology. *Water Res.* **1991**, *25*, 529.
- (42) Straub, T. M.; Pepper, I. L.; Gerba, C. P. *Appl. Environ. Microbiol.* **1992**, *58*, 636.
- (43) Yahya, M. T.; Galsiomes, L.; Gerba, C. P.; Bales, R. C. *Water Sci. Technol.* **1993**, *27*, 409.
- (44) Chiou, C. T.; Kile, D. E.; Rutherford, D. W. *Environ. Sci. Technol.* **1991**, *25*, 660.
- (45) Murphy, F.; Herkelrath, W. N. *Ground Water Monit. Rem.* **1996**, *16*, 86.
- (46) Ryan, J. N.; Gschwend, P. M. *Clays Clay Miner.* **1991**, *39*, 509.
- (47) Yao, K.-M.; Habibian, M. T.; O'Melia, C. R. *Environ. Sci. Technol.* **1971**, *5*, 1105.
- (48) Rajagopalan, R.; Tien, C. *AIChE J.* **1976**, *22*, 523.
- (49) Parks, G. A. In *Equilibrium Concepts in Natural Water Systems*; Stumm, W., Ed.; ACS Advances in Chemistry Series 67; American Chemical Society: Washington, DC, 1967; pp 121–160.
- (50) Aronheim, J. S. Virus Transport in Groundwater: Modeling of Bacteriophage PRD1 Transport through One-Dimensional Columns and a Two-Dimensional Aquifer Tank. M.S. Thesis, Department of Civil, Environmental, and Architectural Engineering, University of Colorado, Boulder, 1995.
- (51) Scholl, M. A.; Mills, A. L.; Herman, J. S.; Hornberger, G. M. *J. Contam. Hydrol.* **1990**, *6*, 321.
- (52) Mills, A. L.; Herman, J. S.; Hornberger, G. M.; DeJesus, T. H. *Appl. Environ. Microbiol.* **1994**, *60*, 3300.
- (53) Tipping, E.; Cooke, D. *Geochim. Cosmochim. Acta* **1982**, *46*, 75.
- (54) Gu, B.; Schmitt, J.; Chen, Z.; Liang, L.; McCarthy, J. F. *Environ. Sci. Technol.* **1994**, *28*, 38.
- (55) Liang, L.; Morgan, J. J. In *Chemical Modeling of Aqueous Systems II*; Melchior, D. C., Bassett, R. L., Eds.; ACS Symposium Series 416; American Chemical Society: Washington, DC, 1990; pp 293–308.
- (56) Tiller, C. L.; O'Melia, C. R. *Colloids Surf. A: Physicochem. Eng. Asp.* **1993**, *73*, 89.
- (57) Amirbahman, A.; Olson, T. M. *Environ. Sci. Technol.* **1993**, *27*, 2807.
- (58) Lance, J. C.; Gerba, C. P. *Appl. Environ. Microbiol.* **1984**, *47*, 484.
- (59) Liang, L.; Morgan, J. J. *Aquat. Sci.* **1990**, *52*, 32.
- (60) Duboise, S. M.; Moore, B. E.; Sagik, B. P. *Appl. Environ. Microbiol.* **1976**, *31*, 536.
- (61) Landry, E. F.; Vaughn, J. M.; Thomas, M. Z.; Beckwith, C. A. *Appl. Environ. Microbiol.* **1979**, *38*, 680.
- (62) Derjaguin, B. V.; Landau, L. D. *Acta Physicochim. URSS* **1941**, *14*, 633.
- (63) Verwey, E. J. W.; Overbeek, J. Th. G. *Theory of the Stability of Lyophobic Colloids*; Elsevier: Amsterdam, 1948.
- (64) Song, L.; Johnson, P. R.; Elimelech, M. *Environ. Sci. Technol.* **1994**, *28*, 1164.
- (65) Small, D. A.; Moore, N. F. *Appl. Environ. Microbiol.* **1987**, *53*, 598.
- (66) Wakamatsu, T.; Fuerstenau, D. W. In *Adsorption from Aqueous Solution*; Weber, W. J., Jr., Matijević, E., Eds.; ACS Advances in Chemistry Series 79; American Chemical Society: Washington, DC, 1968; pp 161–173.
- (67) Dick, S. G.; Fuerstenau, D. W.; Healy, T. W. *J. Colloid Interface Sci.* **1971**, *37*, 595.
- (68) Böhmer, M. R.; Koopal, L. K. *Langmuir* **1992**, *8*, 2649.
- (69) Sivakumar, A.; Somasundaran, P.; Thach, S. *J. Colloid Interface Sci.* **1993**, *159*, 481.
- (70) Schwertmann, U. In *Iron in Soils and Clay Minerals*; Stucki, J. W., Goodman, B. A., Schwertmann, U., Eds.; NATO ASI Series C, Vol. 217; D. Reidel: Dordrecht, 1988; pp 203–250.
- (71) Ruckenstein, E.; Prieve, D. C. *AIChE J.* **1976**, *22*, 276.
- (72) Ryan, J. N.; Gschwend, P. M. *J. Colloid Interface Sci.* **1994**, *164*, 21.
- (73) Ryan, J. N.; Elimelech, M. *Colloids Surf. A: Physicochem. Eng. Asp.* **1996**, *107*, 1.
- (74) Corapcioglu, M. Y.; Haridas, A. *J. Hydrol.* **1984**, *72*, 149.
- (75) Yates, M. V.; Yates, S. R.; Wagner, J.; Gerba, C. P. *J. Contam. Hydrol.* **1987**, *1*, 329.
- (76) Tim, U. S.; Mostaghimi, S. *Ground Water* **1991**, *29*, 251.
- (77) Park, N.-S.; Blanford, T. N.; Huyakorn, P. S. *VIRALT: A model for simulating viral transport in groundwater, Documentation and user's guide, Version 2.1*; HydroGeologic, Inc.: Herndon, VA, 1992.
- (78) Park, N.-S.; Blanford, T. N.; Wu, Y.-S.; Huyakorn, P. S. *CANVAS: A composite analytical-numerical model for viral and solute transport simulation, Documentation and user's guide, Version 1.0*; HydroGeologic, Inc.: Herndon, VA, 1993.

Received for review August 2, 1996. Revised manuscript received October 31, 1996. Accepted November 20, 1996.®

ES960670Y

® Abstract published in *Advance ACS Abstracts*, February 1, 1997.